Memoirs of the Faculty of Engineering, Kyushu University, Vol. 66, No. 3, September 2006

Study on Temperature Dependence of Output Voltage of Electrochemical Detector for Environmental Neutrinos

by

Md Abdul HALIM*, Kenji ISHIBASHI**, Hidehiko ARIMA*** and Norichika TERAO*

(Received August 7, 2006)

Abstract

An electrochemical detector with biological material has been applied for the detection of neutrinos on the basis of a new hypothesis. The detector consisted of two electrodes with raw silk and purified water, and gave an appreciable output voltage. The reproducibility of the experimental results was as good as 99.4% at temperature of 300 K. The temperature dependence of the voltage of the detector was studied at 280, 290, 300 and 310 K. Among them, the detector at 310 K produced the highest output voltage and reached 104 mV in 16 days, whereas that at 280 K generated the lowest voltage and it was as low as 1.2 mV in 16 days. The detectors working at 290 and 300 K produced the voltages 18 and 57 mV in 16 days, respectively. The output voltages of the detector increased with temperature and were in good agreement in spite of the history of temperature. The internal resistance and electromotive force (internal voltage) of the experimental detector were obtained at each temperature by individual analysis and least square fitting method. It was found that the electromotive force was almost constant for these temperatures while the internal resistance showed a large dependence on temperature. The reduction of the output voltage with temperature is dominated by this behavior of internal resistance.

Keywords: Environmental neutrinos, Raw silk, Vector-axial-vector interaction, Conductance, Temperature dependence, Electromotive force and Internal resistance

1. Introduction

Neutrinos are elusive particles with a spin of 1/2, and have no electric charge. Although they are abundant in nature, neutrinos interact with other matter quite weakly. This property makes them extremely difficult to be detected. A number of experiments have been carried out to measure neutrinos through either radiochemical or water Čerenkov approaches[1)-5)]. The radiochemical experiments detect the isotopes that are produced by neutrino-induced reactions on such nuclei as chlorine and gallium during a long exposure period. Water Čerenkov experiments measure the light originating from electrons produced by the elastic scattering reaction. The measured neutrino reaction rates in such neutrino detectors are smaller than the predicted value due to neutrino oscillation[6)]. This suggests that neutrinos should have a quite small mass that differs from zero. However, neutrinos have been treated as a structure-less point particle and no report has clarified their structure so far. It is interesting to consider that neutrinos are not a point-like particle: they are composed of constituent particles and own an internal structure therein. We have made three major assumptions for the constituent particles of neutrinos:

1. Internal interaction potentials are generated by weak dipole moment and weak charge,
2. Motions of neutrino constituent particles are basically governed by an extended Dirac-like equation with vector (V)-axial-vector (AV) matrices, and
3. The neutrino system has internal subspaces for the kinetic motions of constituent particles.

* Graduate Student of Doctor Course, Department of Applied Quantum Physics and Nuclear Engineering
** Professor, Department of Applied Quantum Physics and Nuclear Engineering
*** Research Associate, Department of Applied Quantum Physics and Nuclear Engineering

The hypothesis suggests that an AV auxiliary field like magnetic field in the time direction plays an essential role in keeping the constituent motions and in creating the mass. Some biological materials may create the AV-type field. When the AV-type field of biological material influences low-energy neutrinos, it may induce them to make the transition into the reactive neutrino state. On the basis of this indication[7], we attempted to detect neutrinos with electrochemical detector by the use of biological material of raw silk in the previous study[8),9)]. It was found that the electrochemical detector was capable of responding to both environmental and reactor neutrinos. However, the experiments on detailed characteristics were not performed yet. In the present study, experiments will be carried out to make clear the effect of temperature on the output voltage of the detector, particularly on its temperature-history effect and the behavior of electromotive force (internal voltage) and internal resistance.

2. Detector Principle and Voltage Generation

2.1 Detector principle

Suppose that hydrogen ion (H^+) and hydroxide ion (OH^-) are produced by the dissociation of water molecule. The separation energy[10] is written by $\Delta G = -RT\ln([H^+][OH^-])$, where R is the gas constant, 8.314 J K^{-1} $mole^{-1}$, and T is a temperature typically taken at 300 K. The concentrations of hydrogen ion $[H^+]$ and hydroxide ion $[OH^-]$ are both close to 1×10^{-7} mole per liter purified water. The energy required for the ionic dissociation of water molecule to H^+ and OH^- becomes to 0.84 eV per molecule. This energy is lower than the free energy change (1.23eV) in separation of water molecule into H_2 and $(1/2)O_2$.

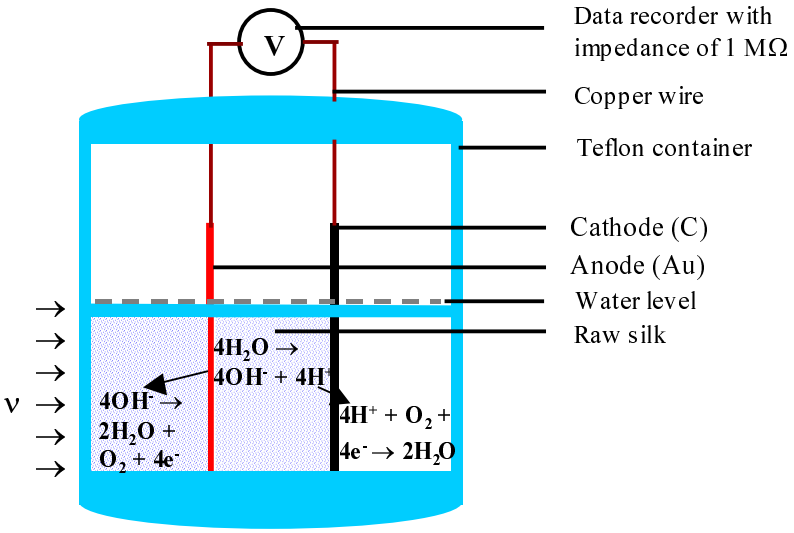

Fig. 1 Principle of voltage generation by the electrochemical method for neutrino detection.

The principle of electrochemical neutrino detection is shown in **Fig. 1**. The AV-field is supposed to be generated by the raw silk, and it may influence the vector (V)-axial-vector (AV) interaction of neutrinos. When the neutrinos transfer some energy above 0.84 eV to water molecules, the water molecules may separate into hydroxyl ions (OH^-) and hydrogen ions (H^+). The OH^- ions migrate to the anode (gold electrode) where free electrons are produced and transferred to the electrode. The electrons move to the cathode through an external conductor. Meanwhile, the H^+ ions diffuse to the cathode (glassy-carbon electrode), and they absorb electrons to form water molecules. The process is described as

Dissociation of water molecule	:	$H_2O \rightarrow OH^- + H^+$
Anode reaction	:	$4OH^- \rightarrow 2H_2O + O_2 + 4e^-$
Cathode reaction	:	$4H^+ + O_2 + 4e^- \rightarrow 2H_2O$.

The current is thus induced in the outer circuit of the detector. Consequently, the voltage of the detector appears.

2.2 Experimental detector

The photographs of the experimental detector together with its parts are shown in **Fig. 2**. Gold and glassy carbon electrodes were used as the cathode and anode, respectively, and they were placed in a cylindrical Teflon container of 90 mm in length and 58 mm in diameter. This container contained 50-g purified water in its lower half region. The dimensions of both gold and glassy carbon electrodes were 20 mm × 50 mm in surface, and the thicknesses of these electrodes were 0.1 mm and 1.0 mm, respectively. The raw silk of 0.5-g was set on the each side of gold electrode, and both electrodes were connected to a voltmeter with impedance of 1 MΩ by the copper wire as shown in **Fig. 1**. The detector was placed in a temperature-controlled incubator. A data recorder was used as a voltmeter in this study. After one cycle of measurement, the experimental data were transferred from the data recorder into a computer by a Communication Unit base of HIOKI 3910.

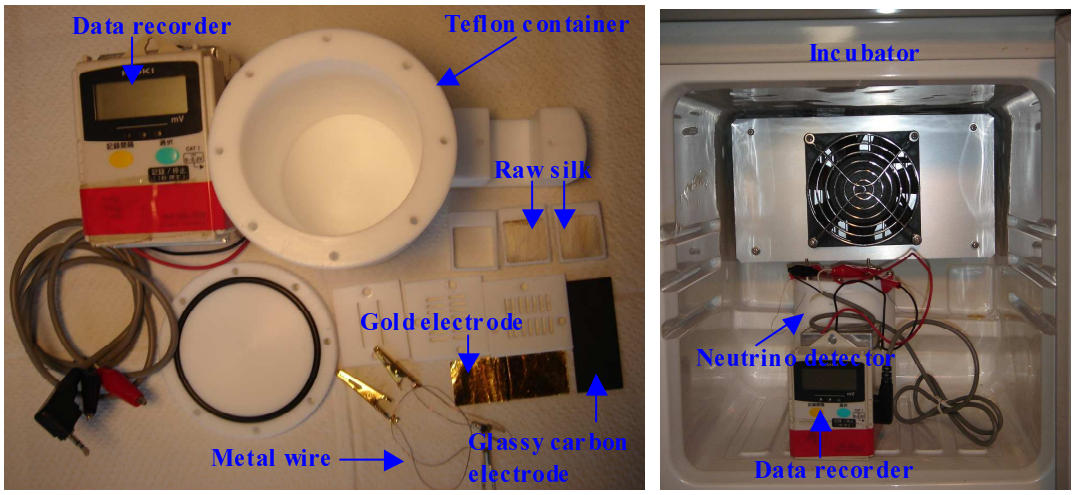

Fig. 2 Photographs of the experimental detector together with its parts (left picture). The detector is placed in an incubator for keeping the temperature constant (right picture).

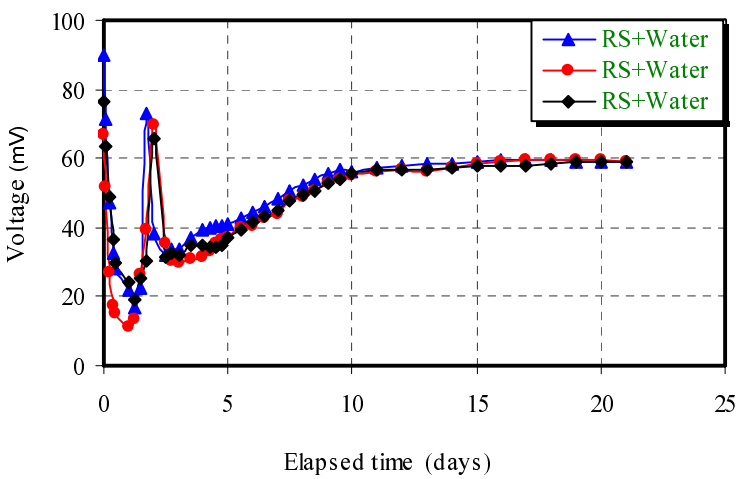

Fig. 3 Output voltages of the detectors with raw silk and purified water operated at 300 K.

2.3 Basic experiment

Three experimental detectors were fabricated with the same composition of 50-g purified water and 1.0-g raw silk to measure the voltage of the detectors. The experiments were conducted at 300 K, and their results are shown in **Fig. 3**. Three detectors produced almost same voltages with elapsed time and the stable voltage reached 58.4 mV in 15 days. The reproducibility of the experiments is as good as 99.4 % after 10 days. The voltage generation in the detector is explained as the function of biological material raw silk existing. The AV-type field is generated by the raw silk in the detector, and this field might influence the vector(V)-axial-vector(AV) interaction of neutrinos. The reactor neutrino experiments confirmed[8)] that the voltage is ascribed to neutrinos incident to the detector.

3. Temperature Dependence

The individual experiments were carried out with the raw silk and purified water at four different temperatures to study the influence of temperature on the voltage of the detector and its reproducibility. The detectors were fabricated with the same composition of 50-g water and 1.0-g raw silk, and operated at temperatures of 280, 290, 300 and 310 K, and all detectors were placed in the temperature-controlled incubator. The experimental results are shown in **Fig. 4**. Typical output voltages are listed in **Table 1**.

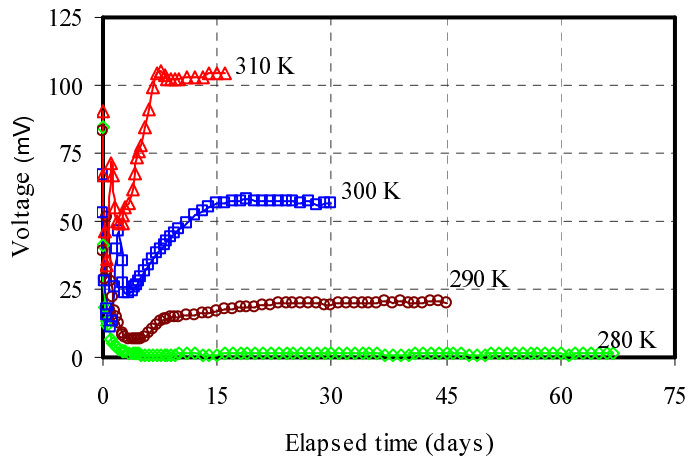

Fig. 4 Voltages of the detectors operated at different temperatures.

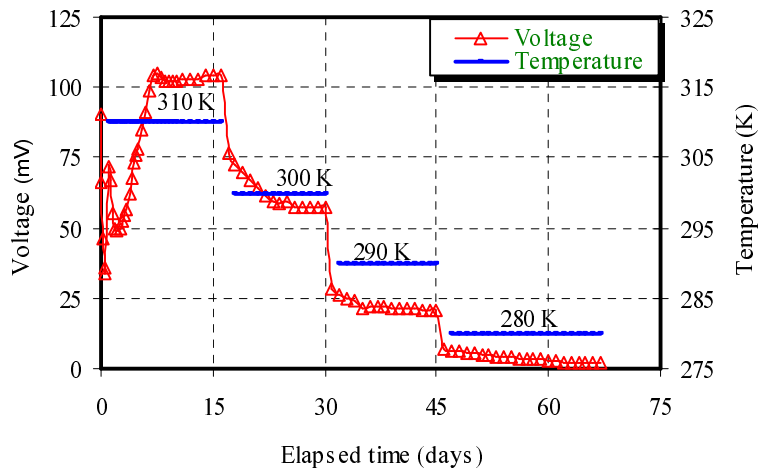

Fig. 5 Output voltages of the detector operated continuously at 310, 300, 290 and 280 K.

The marks in **Fig. 4** stand for the output voltages of the detector at individual temperatures. The voltages of the detectors increased with temperatures. At 310 K, the voltage rises in a higher rate, and shows an equilibrium value after one week. Meanwhile, the voltages of other two detectors, which worked at 300 and 290 K, reach equilibrium states in 2 and 3 weeks, respectively. In contrast, the other one at 280 K produced its voltage as low as about 1 mV after 5 days.

Another continuous experiment was carried out with a temperature variation. The marks in **Fig. 5** show the voltage of this experiment. The detector was initially operated at 310 K for 16 days. At 16 days, the temperature of this detector was decreased from 310 to 300 K. Then, the voltage gradually got lower and reached a stable value. At 30 days again the temperature of the detector was changed from 300 to 290 K and subsequently decreased to 280 K at 45 days. The output voltages are also given in **Table 1**.

Table 1 Comparison between the stable voltages of the detectors operated individually and continuously at different temperatures.

Temperature (K)	Output voltage (mV)	
	Individual experiments (**Fig. 4**)	Continuous experiment (**Fig. 5**)
310	104.4	The same as left
300	56.8	57.5
290	20.0	20.8
280	1.4	1.8

Measured output voltages of the detectors shown in **Figs. 4** and **5** are presented together in **Fig. 6**. Although transient values are different, the voltages converse into the same stable values at each temperature of 300 to 280 K. Equilibrium values are independent of the history.

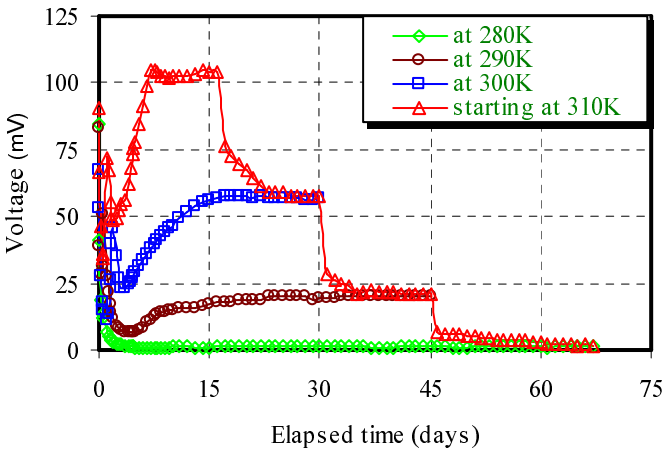

Fig. 6 Comparison between the individual and continuous experimental results.

The temperature makes a great influence on the output voltage of the detector. The conductance is basically proportional to the temperature-dependent function[11] $\exp(-E_\sigma/RT)$, where E_σ is the molar activation energy for transportation. In fact, Iverson made experiments[12] and pointed out that the conductance of pure water and the limiting mobility of H^+ and OH^- increase with temperature.

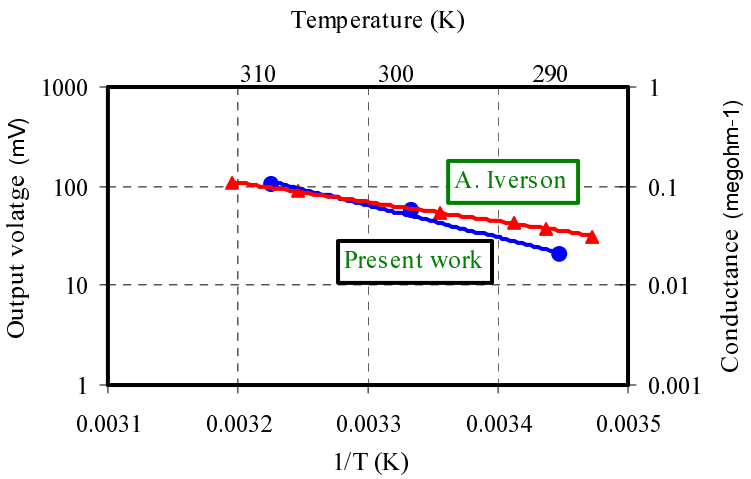

Fig. 7 Comparison between the present experimental output voltages (solid circle) and conductance in a reference for pure water[13] (solid triangle).

Figure 7 shows the comparison between the output voltage of the present experimental detector and conductance of pure water measured by Iverson at different temperatures. From this figure, one can see that the both exponential lines of voltage and conductance increase with temperature. It is interesting to note that the difference between two lines at lower temperature is slightly larger. However, for increasing temperature, the difference becomes less above 300 K.

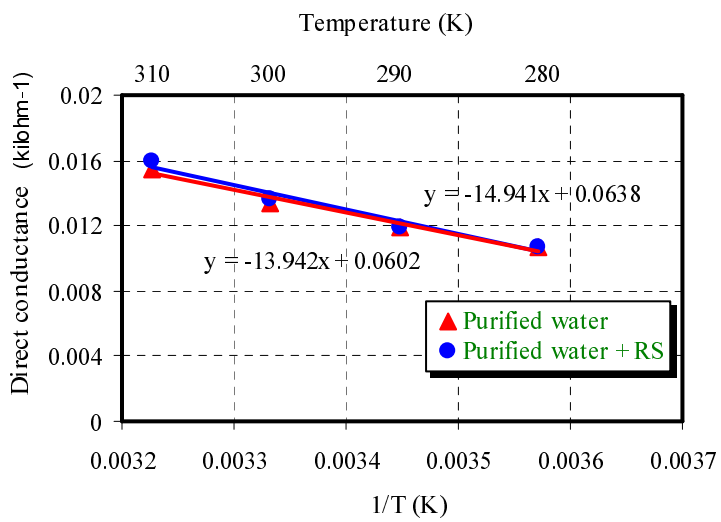

Fig. 8 Conductance of the purified water itself and the water with raw silk directly measured at 280, 290 300 and 310 K with the current of 1 μA.

3.1 Direct conductance measurement at different temperatures

Resistance of the solution of the detector was directly measured with a current of 1 μA at different temperatures. **Figure 8** shows the conductance (direct conductance) of the water with raw silk together with that of the purified water itself. Both linear lines indicate that the conductance increases with temperature and their slopes are almost the same. The conductance of the water with raw silk is slightly higher than the purified water due to some minerals dissolved from raw silk to purified water.

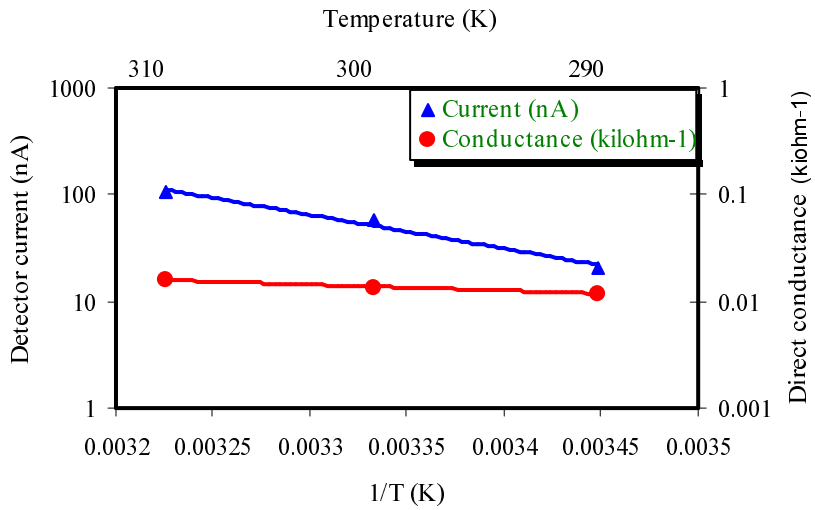

Fig. 9 Comparison between the current of the detector and the directly measured conductance of the purified water with raw silk at different temperatures with the current of 1 μA.

Figure 9 presents the comparison between the detector current and the conductance of water with raw silk measured at 290, 300 and 310 K in this study. Both exponential lines indicate that the current and the conductance increase with temperature. One can see that there is a positive correlation between them in spite of appreciable difference in slope.

3.2 Analysis on electromotive force and internal resistance at different temperatures

The detector owns a definite electromotive forces (internal voltage), which produces open circuit voltage. The detector also has an internal resistance and this resistance reduces the voltage to some extent in operation with a load impedance. To measure this electromotive force and internal resistance, an experiment was carried out according to **Fig. 10** with a parallel circuit. The equivalent resistances R_{eq} of the parallel circuit are obtained by the following equation

$$1/R_{eq} = 1/R_1 + 1/R_2 + 1/R_3, \tag{1}$$

where R_1 and R_2 are the input impedance of data recorder and the resistance of a resistor box, respectively, and R_3 is either resistance of 440 or 2200 kΩ. By using these resistors, the output voltages were measured at 280, 290, 300 and 310 K. The currents i_m were derived from its measured voltages V_m and equivalent resistances R_{eq} at these temperatures as

$$i_m = V_m / R_{eq}. \tag{2}$$

The electromotive force V_{emf} and internal resistance R_{int} of the experimental detector at 280, 290, 300 and 310 K were obtained by using the following equation

$$V_{emf} = R_{\mathrm{int}} i_m + V_m, \tag{3}$$

where V_m and i_m are the measured voltage and current, respectively.

The individually analyzed electromotive force and internal resistance are shown in **Fig. 11**. The individual values have a week dependence on current and are almost constant at each temperature. However, individual electromotive force and internal resistance are obtained in negative values –139.0 mV and –21.0 MΩ at 280 K. When the negative electromotive force divided by the negative internal resistance, it gives positive current then the negative polarity seems to be

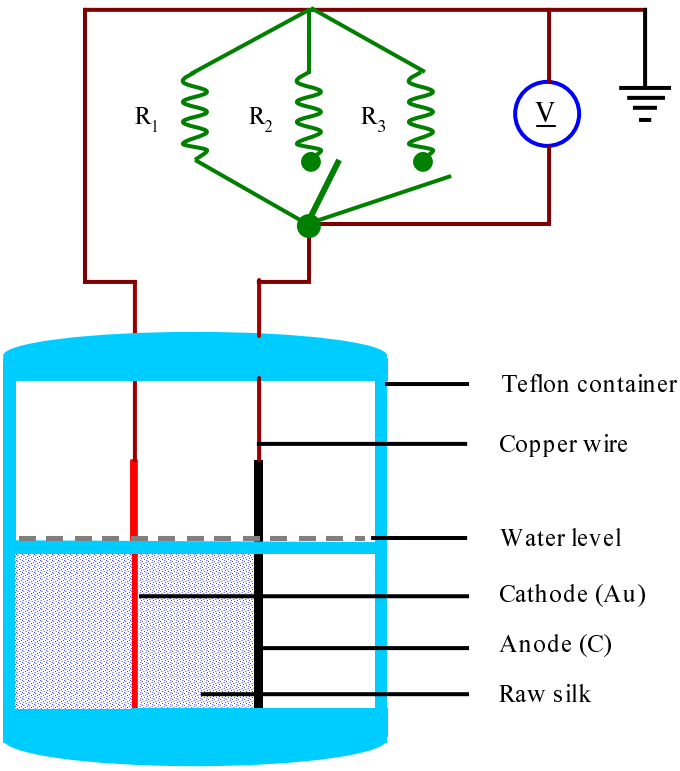

Fig. 10 Schematic diagram for measuring the voltage of the experimental detector with parallel resistances.

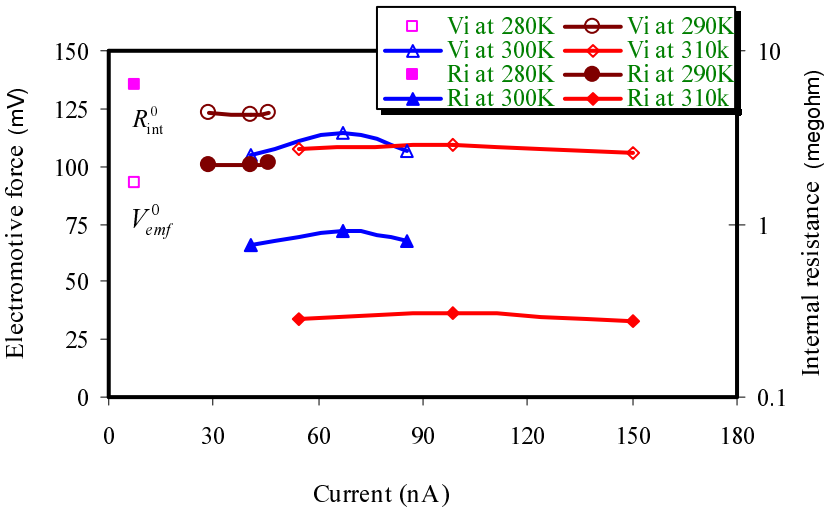

Fig. 11 Individual electromotive force (open marks) and internal resistance (solid marks) of the experimental detector at different currents.

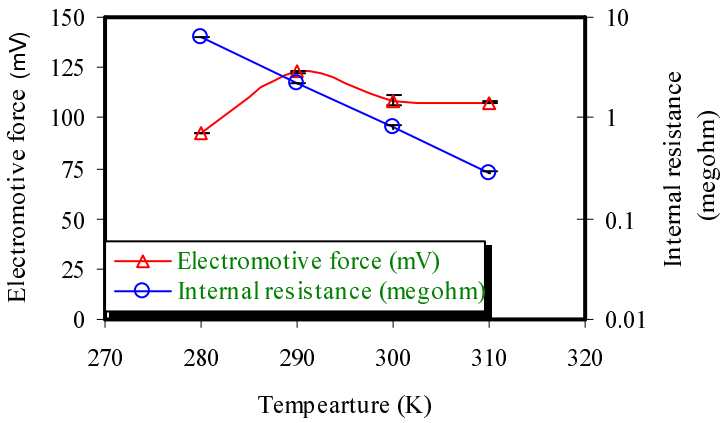

Fig. 12 Average electromotive force and internal resistance of the experimental detectors at 280, 290 300 and 310 K. No error bars are attached for the data at 280 K due to the highly correlated situation.

apparent one. If the current dependent internal resistance is introduced, the negative polarity will be removed. Least square fitting analysis of the electromotive force and internal resistance with their statistical errors are also carried out with SALS. SALS is a general-purpose program package for "Statistical Analysis with Least Squares fitting" with broad range of capabilities. The negative values at 280 K was eliminated by assuming current dependent internal resistance as

$$R_{\text{int}} = R^0_{\text{int}} + F_{\text{int}} i_m, \qquad V^0_{emf} = (R^0_{\text{int}} + F_{\text{int}} i_m) i_m + V_m \tag{4}$$

where R^0_{int} and F_{int} are the intrinsic and co-efficient of internal resistance of the detector, respectively. Although it is possible to make fitting results, the value of V^0_{emf}, R^0_{int} and F_{int} are obtained in a correlated manner. The individually estimated values of electromotive force and internal resistance of the experimental detector are averaged at each temperature. The statistical errors for the average values are estimated with the following equation

$$\sigma = \left(\frac{1}{n} \sum_{i=1}^{n} \left(X_i - \overline{X} \right)^2 \right)^{1/2}, \tag{5}$$

where σ is the statistical error, n is the number of data point, X_i and $\overline{X}$ are the individual and mean values, respectively.

Figure 12 shows the average values of the electromotive force and internal resistance of the experimental detector as a function of temperature. One can see that the electromotive force is not so temperature dependence, but internal resistance of the detector is highly depends on current.

The conductances of the experimental detectors obtained from internal resistances and direct measurements are shown in **Fig. 13** as a function of temperature. The linear straight line for the direct conductance indicates that the charge flow follows the exponential inverse-temperature dependence through the drift of ions having conventional electrons. However, the conductance that was obtained from the internal resistance is quite smaller and highly temperature dependent. This may be ascribed to either surface phenomena on electrodes or volume origin in the water solution. The surface phenomena may come from a small potential difference appearing on the surface of electrode. If the dependence is originating in the volume region, it is supposed that the ions generated by neutrinos includes properties of weak charge and show the behavior unlike the

conventional electrons. Nevertheless, it is surprising that the great change appears in the temperature variation of 20 to 30 degrees.

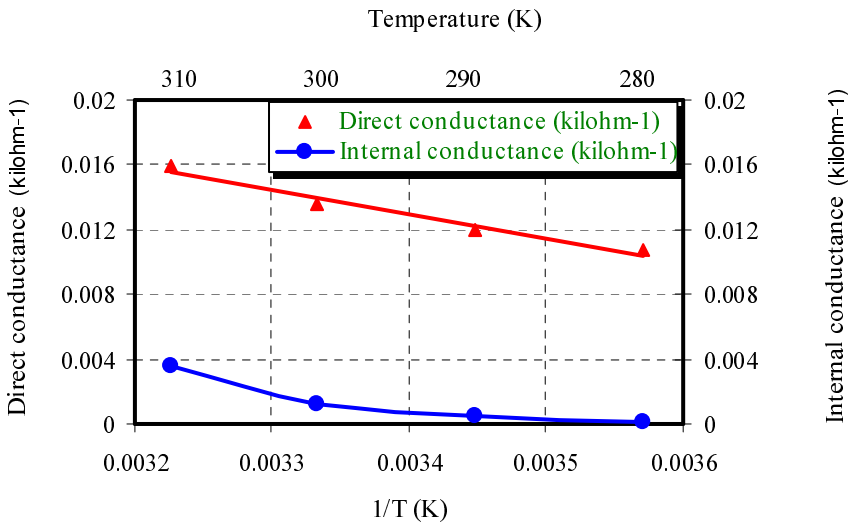

Fig. 13 Comparison between the conductances obtained from direct measurement and internal resistance at 280, 290 300 and 310 K with the current of 1 μA.

4. Conclusion

The temperature exerted a great influence on the output voltage of the detector. The conductance of pure water gets larger with temperature, since the mobility of H^+ and OH^- increases with temperature. Both the measured direct conductances and the output voltages of the detector with purified water and raw silk increased with temperature. This suggested that the voltages of detector increase with temperature since the conductance of the solution gets larger with temperature. The output voltages of the detector increased with temperature and were in good agreement in spite of the history of temperature.

The internal resistance and electromotive force were obtained at 280, 290, 300 and 310 K with the individual analysis and the least square fitting method. The individual values of these quantities were almost constant at each temperature above 290 K. In contrast, the electromotive force and internal resistance were obtained in negative values at 280 K. The negative polarity seems to be apparent one. In fact, the current dependent internal resistance was introduced, and the negative polarity was removed. The electromotive force was basically temperature independent, but internal resistance of the detector highly depended on temperature and did not follow the exponential inverse-temperature dependence at all. This constitutes a major reason for the decrease of the output voltage of the detector with temperature.

References

1) Y. Fukuoda et al., Solar Neutrino Data Covering Solar Cycle 22, Physics Review Letter, 77 1683 (1996).
2) Y. Suzuki et al., 2001 19th International Conference on Neutrino Physics and Astrophysics, Sudbury, Canada, June 2000.
3) M. Altmann et al., GNO Solar Neutrino Observations: Result for GNO I, Physics Letter B, 490, 16 (2000).

4) H. R. Gallagher, Soudan 2 Collaboration, Measurement of the Atmospheric Neutrinos Flavor Ratio in Soudan 2, XVI Workshop on Weak Interactions and Neutrinos, Capri, Italy, June 22-28, 1997.
5) H. B. Li et al., A CsI(Tl) Scintillating Crystal Detector for the Studies of Low-Energy Neutrino Interactions, Nuclear Instruments and Methods in Physics Research A, 459, 93 (2001).
6) I. T. Lawson, Solar neutrino results from he Sudbury Neutrino Observatory, Progress in Particle and Nuclear Physics 48, 5 (2002).
7) Liu Wei et al., Possible Detection of Natural Neutrinos by Use of Small Apparatus, 2nd iTRS International Symposium on Radiation Safety and Detection Technology, Sendai, Japan, July 24-25, (2003).
8) M. A. Halim et al., Detection of environmental neutrinos by electrochemical approach and its pH-vale dependence, Journal of Radiation Protection Bulletin, A special issue, 272 (2005).
9) K. Ishibashi, to be published elsewhere.
10) P. W. Atkins, Physical Chemistry, Oxford University Press (1998).
11) B. W. Rossiter and J. F. Hamilton, Physical methods of chemistry, A Wiley-International publication, 1986, Second edition, Volume II, 692.
12) A. Iverson, The measured resistivity of pure water and determination of the limiting mobility of OH^- from 5 to 550, The Journal of Physical Chemistry, 68, 515 (1964).